Tuning the thermal conductance of molecular junctions with interference effects

J. C. Klöckner,[1,*] J. C. Cuevas,[1,2] and F. Pauly[1,3]

[1]*Department of Physics, University of Konstanz, D-78457 Konstanz, Germany*

[2]*Departamento de Física Teórica de la Materia Condensada and Condensed Matter Physics Center (IFIMAC), Universidad Autónoma de Madrid, E-28049 Madrid, Spain*

[3]*Okinawa Institute of Science and Technology Graduate University, Onna-son, Okinawa 904-0395, Japan*

(Received 16 August 2017; revised manuscript received 19 October 2017; published 21 December 2017)

We present an *ab initio* study of the role of interference effects in the thermal conductance of single-molecule junctions. To be precise, using a first-principles transport method based on density functional theory, we analyze the coherent phonon transport in single-molecule junctions made of several benzene and oligo(phenylene ethynylene) derivatives. We show that the thermal conductance of these junctions can be tuned via the inclusion of substituents, which induces destructive interference effects and results in a decrease of the thermal conductance with respect to the unmodified molecules. In particular, we demonstrate that these interference effects manifest as antiresonances in the phonon transmission, whose energy positions can be tuned by varying the mass of the substituents. Our work provides clear strategies for the heat management in molecular junctions and, more generally, in nanostructured metal-organic hybrid systems, which are important to determine how these systems can function as efficient energy-conversion devices such as thermoelectric generators and refrigerators.

DOI: 10.1103/PhysRevB.96.245419

I. INTRODUCTION

The manipulation of phonon heat conduction at the nanoscale is of fundamental interest for technologies such as thermoelectrics and thermal management in nanoelectronics [1]. Earlier attempts to perform such a manipulation focused on incoherent transport mechanisms, but in recent years and with the advent of nanoscale devices and nanostructured materials, great effort is being devoted to controlling heat currents in the coherent regime by making use of interference effects [2]. Thus, for instance, in the context of phononic structures the so-called superlattices have been introduced. Here one can tune the phonon band structure, phonon group velocity, and the related phonon density of states by means of wave interference effects [3,4]. This strategy is limited by the quality of interfaces in terms of interface roughness and by the mean free path of the heat carriers. Due to these constraints the strategy is, in general, more applicable to systems in which heat is carried by low-energy or, equivalently, long-wavelength phonons. However, if one assumes that atomically thin, single-crystal planes can be manipulated at will, higher-energy or short-wavelength phonons can, in principle, also be affected since structural length scales are of interatomic distance. Thus, Han *et al.* [5] theoretically proposed the suppression of heat transport using defect atoms embedded in a single defect plane. To inhibit the heat flow, the authors exploited the destructive interference between two phonon paths. Resulting line shapes of the energy-dependent phonon transmission are indeed reminiscent of Fano resonances. Such Fano resonances are, in fact, a very general concept in nanostructured materials and occur in every system in which a narrow discrete mode couples to a broad continuous spectrum [6]. Indeed, they have been reported in a great variety of systems ranging from quantum dots to photonic structures [7–9].

Compared to the inorganic materials discussed above, molecules offer an ideal platform to tailor structures at the single-atom level, and single-molecule junctions can be used to probe the coherent transport through the molecules [10]. In the field of molecular electronics, interference effects have been studied with a special emphasis on their impact on the electronic transport properties of such junctions. Theoretically, this topic has been explored extensively in the last two decades [11–27]. In particular, special attention has been devoted to the role of Fano resonances [28–32] and to the determination of general rules governing the appearance of quantum interference effects in molecules with extended π-electron systems [33–36]. Also different experimental reports in recent years have convincingly shown the influence of the quantum interference on electronic transport of molecular junctions, as illustrated by measurements of linear conductances and current-voltage characteristics [37–48]. When comparing electron and phonon transport, it needs to be kept in mind that for electrons the interference has to occur within some $k_B T$ around $\mu \approx E_F$, with E_F being the Fermi energy, to get a measurable effect on the linear conductance. For phonons, instead, Debye energies of typical metal electrodes are in the range of several tens of meV so that a sizable window of phonon energies already contributes to thermal transport at room temperature.

In the case of coherent phonon transport in molecular junctions the impact of interference effects is starting to be analyzed theoretically [49,50]. For instance, Markussen [49] investigated the role of phonon interference in molecular junctions made of benzene and oligo(phenylene ethynylene) (OPE3) molecules attached to Si and graphene nanoribbon electrodes. Combining *ab initio* calculations for vibrational properties of the molecules with a phenomenological description of the leads and the molecule-lead couplings, Markussen found that the phonon transmission function for cross-conjugated molecules, like meta-connected benzene, exhibits destructive interference features very similar to those

*jan.kloeckner@uni-konstanz.de

found for the corresponding electronic transport, which cause a reduction of the phononic thermal conductance with respect to the linearly conjugated analogs. On the other hand, Famili *et al.* [50] studied the phonon transport in alkane chains by means of a first-principles method based on density functional theory (DFT). In particular, they investigated the appearance of Fano resonances, when the alkanes are modified by the inclusion of certain side groups, so-called Christmas trees. These resonances led to a reduction of the corresponding thermal conductance by a factor of 2. However, alkanes are known to exhibit geometrical gauche defects that result in the localization of vibrational modes. These defects have been reported to reduce the thermal conductance by a similar magnitude [51], making it presumably difficult to discriminate between the effects of side groups and gauche defects. In this sense, the study of stiff molecules like benzene derivatives may provide more conclusive results about the existence of interference effects.

In this work we employ a full *ab initio* DFT-based transport method to study the role of phonon interference effects in the thermal conductance of single-molecule junctions. In particular we explore benzene- and OPE3-related molecules, but contrary to Ref. [49], we assume that the electrodes are made of Au, which is often the material of choice for the leads of molecular junctions, and use amine anchoring groups. In the case of benzenediamine we find that due to the small Debye energy of Au of around 20 meV, no destructive interference effects are visible in the phonon transmission function, irrespective of whether the molecule is contacted to Au in a para or meta configuration. This leads to a room-temperature thermal conductance that is similar for the two contacting schemes. More importantly, we show that this situation can be changed by replacing a H atom of benzene by a halogen atom (F, Cl, Br, I). The substitution may lead to a reduction of the thermal conductance by up to a factor of 1.7. We also show that by increasing the number of substituent atoms in the benzene molecule and depending on their precise position on the ring, one can induce additional reductions of the thermal conductance by a factor of 2.5. Finally, we also show that similar concepts apply to the case of OPE3, and in particular, we find a clear difference between para- and meta-OPE3, where the central benzene ring is connected in the para or meta position. Our work provides concrete predictions that can potentially be tested, given the recent experimental advances in the measurement of the thermal conductance of atomic-scale contacts [52,53]. In addition, it sheds light on the importance of phonon interference effects to tune the thermal transport of molecular junctions.

The rest of this paper is organized as follows. In Sec. II we briefly describe the theoretical techniques employed in this work to study the phonon transport in single-molecule junctions. In Sec. III we present the main results of this work concerning the phonon thermal conductance of single-molecule junctions based on benzene and OPE3 derivatives. We summarize our main conclusions in Sec. IV. Finally, we discuss in the Appendix our results for the electronic thermal conductance of the molecular junctions studied in this work to show that the thermal transport is actually dominated by phonons.

II. THEORETICAL METHOD

To explore the influence of phonon interference on the thermal conductance of single-molecule junctions, we describe coherent phonon transport within the Landauer-Büttiker approach. This approach is based on the harmonic approximation and is valid if the characteristic dimensions of the atomic-scale junction are smaller than the inelastic mean free path for phonons, which is on the order of a few nanometers at room temperature for gold [54]. The main source of resistance is then the elastic scattering in the narrowest part of the device. Thermalization due to third- or higher-order interactions between atoms that lead to phonon-phonon scattering is assumed to take place exclusively in the electrodes, which are thus treated as reservoirs with a well-defined thermodynamic state.

Within this approach the linear thermal conductance due to phonons is given by

$$\kappa_{\mathrm{pn}}(T) = \frac{1}{h}\int_0^\infty dE\, E\,\tau_{\mathrm{pn}}(E)\frac{\partial n(E,T)}{\partial T}, \tag{1}$$

where $n(E,T) = [\exp(E/k_{\mathrm{B}}T) - 1]^{-1}$ is the Bose function and $\tau_{\mathrm{pn}}(E)$ is the energy-dependent phononic transmission. We compute the transmission function $\tau_{\mathrm{pn}}(E)$ by means of a combination of DFT and nonequilibrium Green's function techniques, as we have described in detail in Refs. [55–57].

Briefly, the first step in the calculation is the construction of the molecular junction geometries. For this purpose, we use DFT to obtain equilibrium geometries through total-energy minimization. From these calculations the vibrational properties in terms of the dynamical matrix are obtained by applying density functional perturbation theory, as implemented in the quantum chemistry software package TURBOMOLE 6.5 [58–60]. In our DFT calculations we employ the Perdew-Burke-Ernzerhof exchange-correlation functional [61,62], the basis set of split-valence-plus-polarization-quality def2-SV(P) [63], and the corresponding Coulomb fitting basis [64]. In order to accurately determine the force constants and related vibrational energies, we use very strict convergence criteria. In particular, total energies are converged to a precision of better than 10^{-9} a.u., whereas geometry optimizations are performed until the change of the maximum norm of the Cartesian gradient is below 10^{-5} a.u. We have checked that our stringent convergence criteria avoid the appearance of any modes with imaginary frequencies in the optimized junction region, which would otherwise signal unstable geometries. It is furthermore worth stressing that in our method the electrodes are described by means of perfect semi-infinite crystals, whose phonon properties are determined within DFT with the same functional and the same basis set as used for the central device part. In this way we achieve a consistent, full *ab initio* treatment of the phonon system of the whole molecular junctions. Finally, the dynamical matrix of the molecular junction is used to compute the phonon transmission function with the help of nonequilibrium Green's function techniques, as presented in Ref. [55].

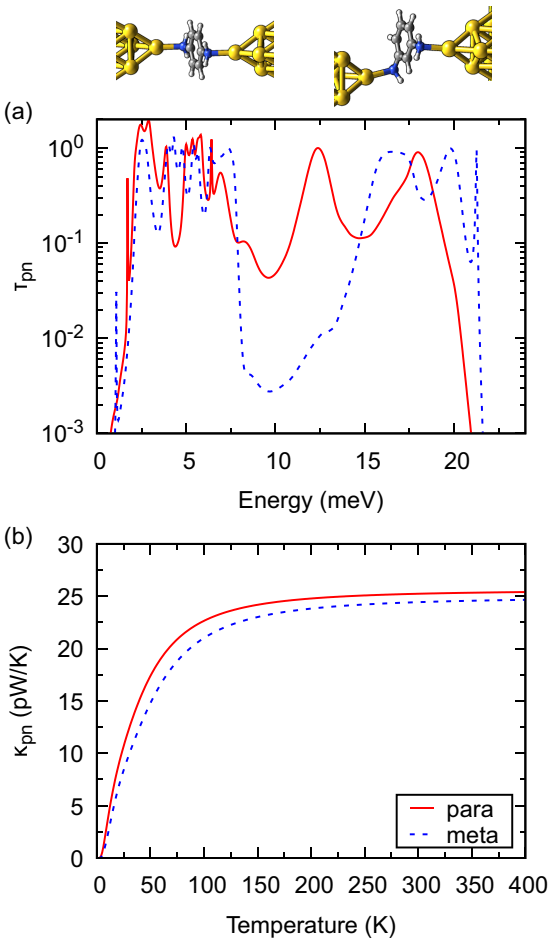

FIG. 1. (a) Phonon transmission as a function of energy for the Au-benzenediamine-Au junctions shown above the panel for both para (left) and meta (right) binding configurations. (b) The corresponding phononic thermal conductance as a function of temperature.

III. RESULTS

We start our discussion of the results with an analysis of single-molecule junctions based on the unsubstituted benzenediamine molecule. As shown in the top part of Fig. 1, we consider contacts, where the amino (NH_2) group is attached to a single tip atom of the gold electrodes on each side in both the para and meta configurations. We will refer to this amino binding site on gold also as the "atop position" and note that these geometries are similar to those used in previous studies of electronic transport, mimicking typical binding geometries [65]. In Fig. 1(a) we show the results for the phononic transmission of these two binding configurations, computed with our *ab initio* method, described in the previous section. The first thing to notice is that the transmission is finite only below approximately 20 meV, which corresponds to the Debye energy of the gold electrode material. On the other hand, notice that although both transmission curves are different, which is reasonable due to the different geometrical configurations, we do not find any signature of destructive interference in the form of antiresonances. This is further confirmed by the results for the temperature dependence of the phononic thermal conductance, which we show in Fig. 1(b). In fact, both molecules exhibit similar thermal conductance values over the whole temperature range explored here.

The reason for the lack of destructive interference effects in these benzene-based junctions can be understood with the help of the work of Markussen [49]. Considering his semiempirical results for phonon transport in benzene junctions with Si electrodes, he found that the lowest observable destructive interference features appear at energies around 40 meV. Since this energy is above the Debye energy of gold, no effects are visible in our case.

These results raise the question of whether it is possible to observe interference effects in the phonon transport in junctions based on benzene derivatives with the standard Au leads. In the context of electronic transport it is known that interference features can be shifted in energy by introducing side groups [22], which have either electron-withdrawing or electron-donating character. The inclusion of such side groups moves the resonance features to lower or higher energies, respectively. Furthermore, the substituents can also break the symmetry of the molecule, leading to destructive interference in benzene junctions even for the para configuration of anchoring groups. Inspired by this idea, we analyze in what follows the effect of substituting a H atom in the benzenediamine molecule by a heavier atom of mass m to tune the position of the resonance features. The basic idea is to try to shift the destructive resonances below the Debye energy of gold to observe a measurable effect on the thermal conductance.

With this idea in mind we consider the phonon transport in Au-benzenediamine-Au single-molecule junctions, where one of the H atoms of the benzene has been substituted by a halogen atom X = F, Cl, Br, I, as depicted in the upper part of Fig. 2. The naive expectation is that since the energy of a harmonic oscillator scales as $E \propto \sqrt{k/m}$, with k being the force constant, the resonance features should decrease in energy with increasing mass m of the substituent from F to I. This simple view is indeed confirmed by our *ab initio* calculations of the phononic transmission, which are summarized in Fig. 2(a) for the substituted benzenediamine molecule in the para configuration. As one can see, there is a clear destructive interference feature for X = Br at an energy of around 19 meV. It is further shifted to lower energies for X = I, where it appears at around 16 meV. Additionally, we see that the peak at around 13 meV for the unsubstituted benzenediamine shifts to lower energies as the mass of the substituent increases, while the transmission for energies lower than 10 meV remains nearly unaffected. These results for the transmission have a clear impact on the phononic thermal conductance [see Fig. 2(b)]. Notice, in particular, that the thermal conductance decreases monotonically with the mass of the substituent, reaching in the case of X = I a reduction factor of 1.7 at room temperature, compared with the unsubstituted benzene molecule.

To assess in a quantitative manner the impact of the antiresonances on the reduction of the thermal conductance upon the introduction of substituents, it is useful to investigate the so-called cumulative thermal conductance,

$$\kappa^{c}_{pn}(E,T) = \frac{1}{h}\int_0^E dE'\, E'\tau_{pn}(E')\frac{\partial n(E',T)}{\partial T}, \qquad (2)$$

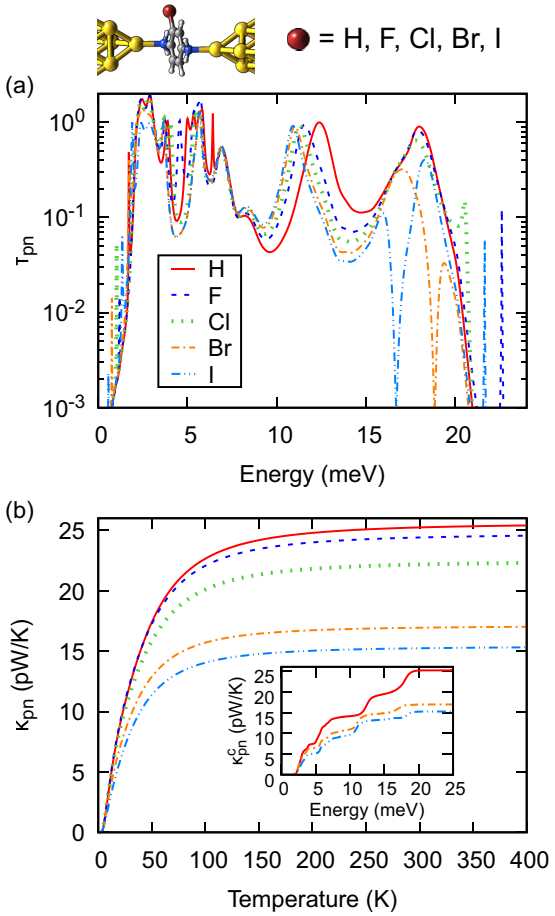

FIG. 2. (a) Phonon transmission as a function of energy for Au-benzenediamine-Au junctions, where a H atom of the benzene molecule has been substituted by a halogen atom (X = F, Cl, Br, I); see the diagram at the top. (b) The corresponding phononic thermal conductance as a function of temperature for the different benzenediamine derivatives. The inset shows the room-temperature cumulative thermal conductance as a function of energy for the junctions with X = H, Br, I.

which is defined as the thermal conductance due to phonon modes up to a given energy E. We show in the inset of Fig. 2(b) the room-temperature cumulative thermal conductance as a function of energy for the Au-benzenediamine-Au junctions with X = H, Br, I. As we can see, the introduction of substituents actually modifies the phonon transport at all energies, but the change is particularly drastic at the energies at which the antiresonances occur. This illustrates that the destructive interference effects, induced by substituent atoms, play a key role in the reduction of the heat transport and can be used as a strategy to modify the thermal conductance.

In order to understand the origin of the destructive interference effect, discussed above for Br and I, we follow an argument based on the symmetry of the molecular orbitals developed for electron transport [33]. Since the structure of the transport formalism is almost identical for electrons and phonons, with the only difference arising from the equations of motion, this argument can be straightforwardly adapted to phonon transport. Assuming for simplicity only nearest-neighbor couplings, the idea is as follows. If the molecule is attached to the left lead at position l with coupling constant k_{lL} and at position r with coupling constant k_{rR} to the right lead, then the transmission function can be expressed as

$$\tau_{\mathrm{pn}}(E) = \frac{\pi^2}{E^2} k_{\mathrm{lL}}^2 k_{\mathrm{rR}}^2 \rho_{\mathrm{L}}(E)\rho_{\mathrm{R}}(E)|D_{\mathrm{lr}}(E)|^2. \tag{3}$$

Here $\rho_\alpha(E)$ is the local density of states at the lead atom α = L,R that is connected to atom l,r of the molecule, respectively, and $D_{\mathrm{lr}}(E)$ is the lr-matrix element of the Green's function at energy E. Let us assume that the typical embedding self-energies $\Pi_\alpha(E)$, which describe the coupling of the central junction part to the left and right electrodes [55,56] and appear in the full expression for $D_{\mathrm{lr}}(E)$, can be neglected, which is, for instance, the case if molecule-lead couplings are not too strong. In this situation the Green's function entering in the previous equation can be approximated by the corresponding Green's function of the isolated molecule. It is given by the following spectral representation:

$$D_{\mathrm{lr}}(E) = \sum_j \frac{C_{\mathrm{l}j} C^*_{\mathrm{r}j}}{(E+i\eta)^2 - E_j^2}, \tag{4}$$

where C_{nj} is the nth component of the jth eigenfunction or vibrational mode. Given the dynamical matrix $\boldsymbol{K}$, the eigenfunctions C_{nj} and angular momentum frequencies ω_j are obtained by solving the secular equation

$$\boldsymbol{K}\boldsymbol{C}_j = \omega_j^2 \boldsymbol{C}_j. \tag{5}$$

In the spectral representation in Eq. (4), η is a small imaginary part that prevents $D_{\mathrm{lr}}(E)$ from diverging at $E \to E_j$, and $E_j = \hbar\omega_j$ is the energy of the jth vibrational mode of the isolated molecule. As discussed in Ref. [33] for molecular junctions and in Ref. [66] for mesoscopic systems, a destructive interference occurs between vibrational modes j that exhibit the same sign of the product $C_{\mathrm{l}j}C^*_{\mathrm{r}j}$ or, more pictorially, the same parity of vibrational modes at the lead-connecting molecular sites. This conclusion is obvious from the general form of the Green's function in Eq. (4). If the embedding self-energies $\Pi_\alpha(E)$ are taken into account, they may lead to renormalizations of level positions and hence antiresonance peaks. They are also important to describe level broadenings, which are mimicked in Eq. (4) by η, and hence to avoid any divergencies of the transmission in Eq. (3) at resonance positions $E = E_j$.

Let us now apply these ideas to understand the antiresonance that appears at around 19 meV in the transmission function for the benzenediamine junction with the substituent X = Br [see Fig. 2(a)]. For this purpose we first analyzed the vibrational modes of the isolated molecule within DFT and identified the two modes at 15.61 and 20.07 meV, which are shown at the top of Fig. 3. Taking into account only these two modes in the sum over j in Eq. (4), we also display in Fig. 3 the corresponding absolute value of $D_{\mathrm{lr}}(E)$. Here the connection to the leads has been assumed to be established only at the N atoms, and the coefficients C_{nj} have been taken from the calculations of the isolated molecule. Since these two modes exhibit the same oscillation direction on the N atoms, the products $C_{\mathrm{l}1}C^*_{\mathrm{r}1}$ and $C_{\mathrm{l}2}C^*_{\mathrm{r}2}$ have the same sign, and modes 1 and 2 are expected to interfere destructively. This is

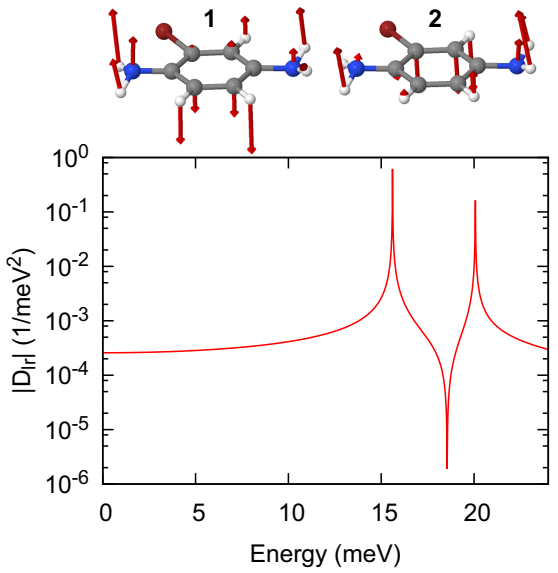

FIG. 3. In the diagrams at the top we visualize the two modes, 1 and 2, that are responsible for the destructive interference feature at 19 meV in the benzenediamine molecule, substituted with $X = \mathrm{Br}$. The first mode is at an energy of 15.61 meV, and the second one is at 20.07 meV. Since for both modes the arrows on the N atoms on the left and right sides point in the same direction, they interfere destructively. The graph below shows the calculated absolute value of the relevant Green's function element of the isolated molecule, taking into account in Eq. (4) only modes 1 and 2 and using $\eta = 10^{-3}$ meV.

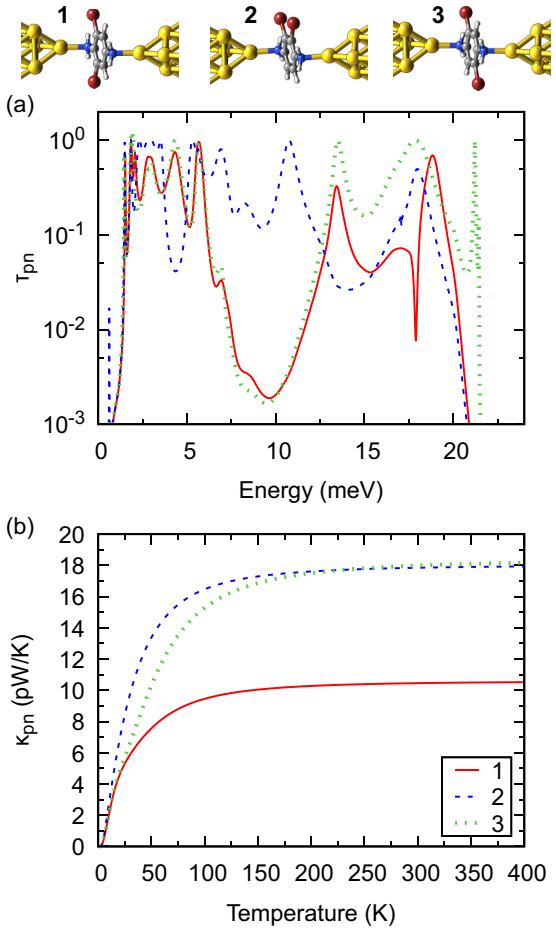

FIG. 4. (a) Phonon transmission as a function of energy for the three molecular junctions shown above, where two H atoms of the benzenediamine molecule have been replaced by two Br atoms. (b) The corresponding temperature dependence of the phononic thermal conductance.

confirmed by the behavior of $|D_{\mathrm{lr}}(E)|$ in Fig. 3, which exhibits two peaks at the energies of the two modes and a minimum at around 19 meV, energetically located between these two modes. The position of the minimum is in good agreement with the minimum in the transmission curve in Fig. 2. Let us mention that the same considerations apply for the molecule with $X = \mathrm{I}$, where we find two modes of similar characteristics at energies around 14.7 and 19.5 meV.

One may wonder whether the antiresonances, resulting from destructive interference, survive upon the elongation of the molecular junctions. We have investigated this aspect for the junctions with the benzene derivatives studied in Fig. 2 and found that the appearance of antiresonances is quite robust against stretching or compression. This is indeed expected since, as we have discussed above, the antiresonances originate from the interference of internal vibrational modes of the molecules, and they are therefore not greatly affected by variations of the distance between the electrodes.

Following the analogy with electronic systems, we analyze now how the inclusion of additional substituents modifies the interference patterns [36]. For this purpose we investigate the phonon transport through benzenediamine junctions if two H atoms are replaced by two Br atoms. Moreover, we study the influence of the exact position where these Br atoms are incorporated and examine the three molecular junctions shown at the top of Fig. 4. All vibrational modes between 15 and 20 meV in the central region of the corresponding junctions are shown in Fig. 5.

The results for the phonon transmission are displayed in Fig. 4(a). As one can see, for molecule 1 a destructive interference antiresonance appears at about 17 meV. The origin of this feature is, like for the previous compounds, the interference between two modes that lie close in energy. These are the modes with energies of 17.75 and 18.95 meV in the left column of Fig. 5 that show the same parity on the terminal N atoms of the molecule. The difference with respect to the singly substituted molecules discussed above is that these modes have no analogs in the isolated molecule. Instead, they are hybrid modes in the sense that they also involve vibrations of the gold atoms in the electrodes. Additionally, a reduced transmission peak at 12.5 meV arises which is due to a localized mode that is asymmetrically coupled to the electrodes. Interestingly, the other two molecules, 2 and 3, do not exhibit any pronounced antiresonance, resulting from destructive interference [see Fig. 4(a)], which we attribute to the lack of the necessary symmetry of the vibrational modes on the terminal N atoms (see Fig. 5). This shows that not only the masses of the substituents play a role, but so does the exact position, where they are introduced. The changes in the transmission are reflected in the corresponding thermal conductance results. As we see in Fig. 4(b), while molecule

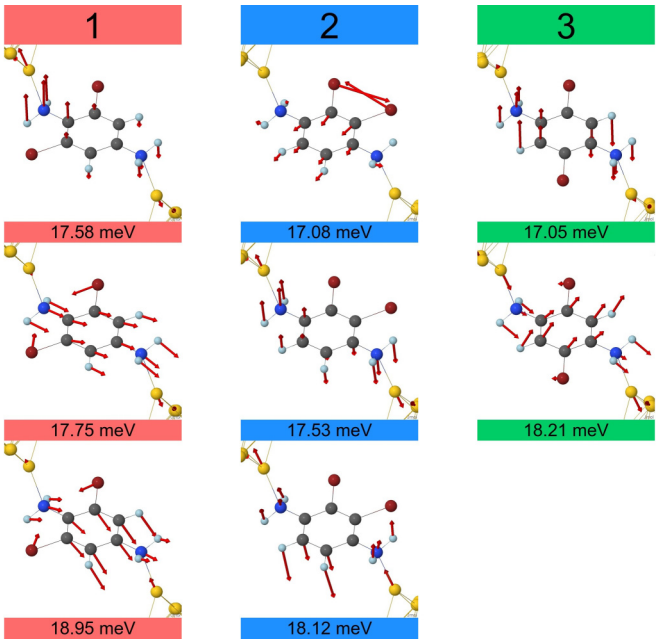

FIG. 5. All vibrational modes in the central region of the three molecular junctions discussed in Fig. 4 in the energy range between 15 and 20 meV.

1 exhibits a largely reduced thermal conductance at room temperature compared to both the singly substituted case and the unsubstituted benzenediamine, molecules 2 and 3 exhibit conductance values that are similar to those of the singly substituted case.

Now we show that the basic concepts discussed above also apply to other, more complex molecules. For this purpose, we consider OPE3. This molecule has been analyzed in the context of phonon transport in Ref. [49] with the help of semiempirical methods and considering Si as well as graphene-nanoribbon electrodes. First, we discuss the influence of the binding configuration by examining para- vs meta-OPE3, as shown at the top of Fig. 6. In this case our *ab initio* results for the phonon transmission, which are displayed in Fig. 6(a), show that for meta-OPE3 several resonance peaks at energies below 15 meV appear to be shifted to lower energies compared to para-OPE3, while there is a pronounced decrease of the transmission for the meta-OPE3 above. The strong suppression of the transmission at around 18 meV is due to an interference effect in which two quasidegenerate modes are involved, as explained in Ref. [49]. In total the meta-OPE3 thermal conductance is reduced by a factor of 2 compared to that of para-OPE3.

As in the case of benzene, the thermal conductance of Au-OPE3-Au junctions can be tuned by substituting one H atom in the central benzene ring with a halogen atom, as sketched in the diagram at the top of Fig. 7. Similar to benzenediamine in Fig. 2, one can see in Fig. 7(a) that the phonon transmission exhibits an antiresonance at energies around 15–20 meV for the substituents Br and I, but now this feature also appears for Cl. Again, the occurrence of destructive interferences below the Debye energy of gold leads to a suppression of the corresponding thermal conductance, as we show in Fig. 7(b). We find a monotonically decreasing thermal conductance with increasing mass of the substituent.

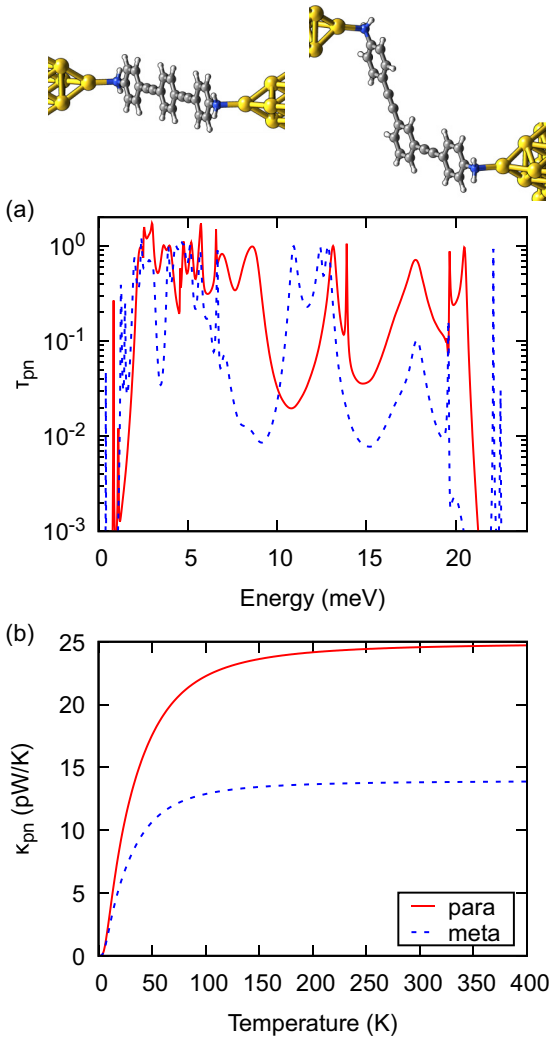

FIG. 6. (a) Phonon transmission as a function of energy for the Au-OPE3-Au junctions shown above for both para (left) and meta (right) binding configurations at the central benzene ring. (b) The corresponding phononic thermal conductance as a function of temperature.

As in the case of the benzene derivatives, this behavior is due to the fact that, upon introducing the substituents, the energies of the vibrational modes decrease, and the antiresonances, resulting from the interference effects, are redshifted at the same time.

Let us mention that we are not aware of the exact OPE3 compounds, shown in Fig. 7, having been synthesized. But closely related molecules exist in which the central ring of an OPE3 diamine has been modified, among other things, by the inclusion of several fluorine atoms and which have been studied in the context of single-molecule junction experiments [67]. So we think that there should not be any fundamental problem to synthesizing the compounds discussed in this work. In this respect, it is also worth stressing that our DFT calculations demonstrate that these molecules are indeed stable

To conclude the discussion of our results on phonon heat transport, it is important to emphasize that in all the molecular junctions investigated in this work, the room-temperature

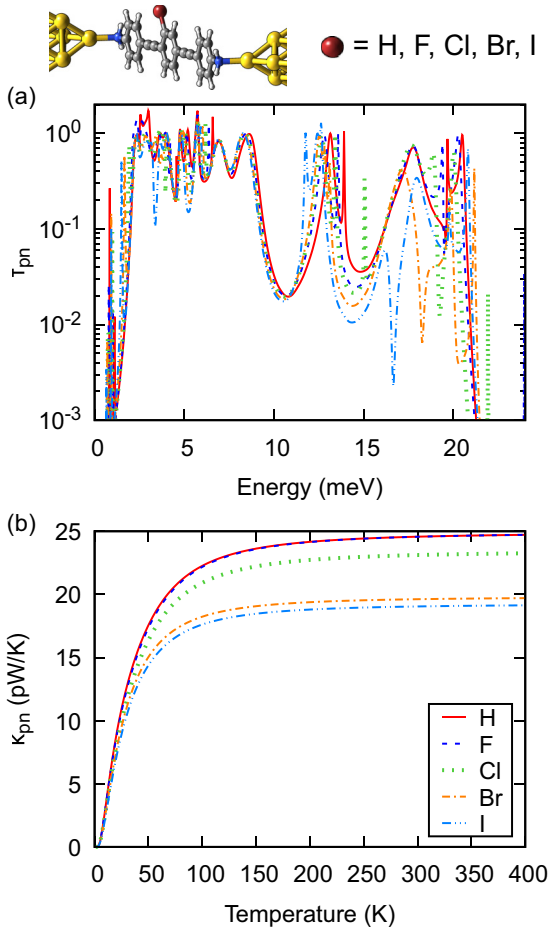

FIG. 7. (a) Phonon transmission as a function of energy for Au-para-OPE3-Au junctions, where a H atom of the central benzene ring has been substituted by a halogen atom (X = F, Cl, Br, I); see diagram above. (b) The corresponding phononic thermal conductance as a function of temperature for the different para-OPE3 derivatives.

thermal conductance is dominated by the contribution of phonons. Therefore, the impact of the interference effects discussed here should be, in principle, amenable to measurement. This point is discussed in detail in the Appendix, where we present our results for the electronic contribution to the thermal conductance.

IV. CONCLUSIONS

Making use of a full *ab initio* transport method, we have analyzed the influence of phonon interference on the thermal conductance of benzene and OPE3 derivatives attached to Au electrodes via amino groups. We have found that for unsubstituted benzene no interference effects are visible, irrespective of the binding configuration, which is due to the small Debye energy of gold. We have also shown that substitution of one H atom with a halogen atom of increasing mass leads to the appearance of Fano-like resonances at energies below the Au Debye energy, which in turn leads to a reduction of thermal conductances by up to a factor of 1.7. We were able to relate this kind of antiresonance feature to the destructive interference between two modes of the free molecule with the same symmetry in the region where the molecule is connected to the leads. We have also shown that the thermal conductance can be further reduced by increasing the number of substituent atoms and arranging them in appropriate positions.

Finally, we have used similar concepts to tune the thermal conductance of junctions based on OPE3 molecules. In particular, we have demonstrated that the thermal conductance of meta-OPE3 junctions is clearly reduced compared to the para-OPE3 case mainly due to interference between two quasidegenerate vibrational modes. On the other hand, we have also shown that the thermal conductance of a linear Au-OPE3-Au junction can be reduced by incorporating halogen atoms in the central ring of this molecule. Again, this effect is due to the appearance of destructive phonon interference.

In summary, we have demonstrated that, in analogy to the electronic transport, the thermal conductance of molecular junctions can be controlled by means of phonon interference effects. Even if the effect for phonons is not as dramatic as for the electronic analog, our findings are important to achieve heat management in nanostructured metal-molecule hybrid systems and to explore their potential in thermoelectric applications.

ACKNOWLEDGMENTS

J.C.K. thanks A. Irmler for stimulating discussions. J.C.K. and F.P. gratefully acknowledge funding from the Carl Zeiss Foundation and the Junior Professorship Program of the Ministry of Science, Research, and Arts Baden-Württemberg. J.C.C. is supported by the German Research Foundation (DFG) and the Collaborative Research Center (SFB) 767, which sponsor his stay at the University of Konstanz as a Mercator Fellow, as well as the Spanish Ministry of Economy and Competitiveness (Contract No. FIS2014-53488-P). An important part of the numerical modeling was carried out using the computational resources of the bwHPC program, namely, the bwUniCluster and the JUSTUS HPC facility.

APPENDIX: ELECTRONIC THERMAL CONDUCTANCE

In this Appendix we briefly discuss our results on the electronic contribution to the thermal conductance for the different molecular junctions investigated in this work. The goal is to show that in these junctions the thermal transport is dominated by phonons and that the interference effects, predicted here, should therefore be observable experimentally. We neglect contributions to the thermal conductance from near-field radiative heat transfer, whose significance can be controlled by the macroscopic shape of the electrodes [57].

As in the phononic case we assume that the electronic transport is dominated by elastic tunneling processes. Thus, we compute the electronic contribution to the thermal conductance in the linear response regime within the Landauer-Büttiker formalism. It is given by [10]

$$\kappa_{el}(T) = \frac{2}{hT}\left(K_2(T) - \frac{K_1(T)^2}{K_0(T)}\right), \qquad \text{(A1)}$$

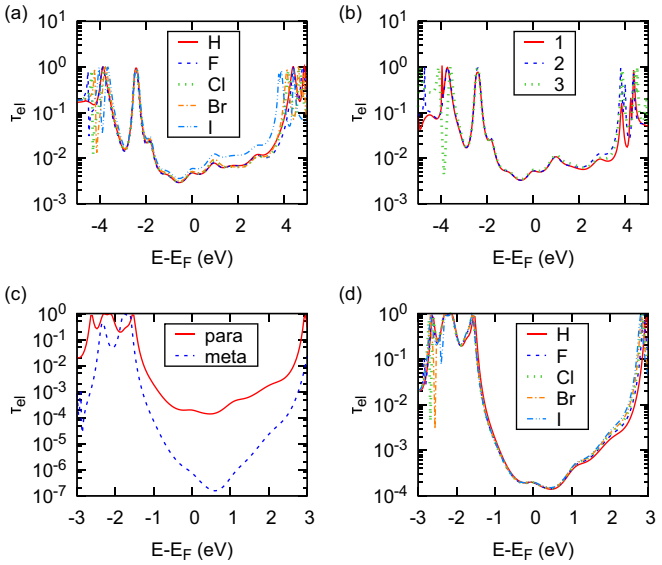

FIG. 8. Electronic transmission as a function of energy, computed for (a) the molecular junctions of Fig. 2 based on benzene with a single halogen atom as substituent, (b) the junctions of Fig. 4 based on benzene with two Br atoms as substituents, (c) the para- and meta-bonded OPE3 junctions of Fig. 6, and (d) the OPE3-based junctions of Fig. 7 with a single substituent on the central benzene ring.

where the coefficients are defined as

$$K_n(T) = \int_{-\infty}^{\infty} dE\, \tau_{el}(E)\left(-\frac{\partial f(E,T)}{\partial E}\right)(E-\mu)^n, \quad \text{(A2)}$$

$\tau_{el}(E)$ is the energy-dependent electron transmission, and $f(E,T) = \{\exp[(E-\mu)/k_BT]+1\}^{-1}$ is the Fermi function. Here, the chemical potential $\mu \approx E_F$ is approximately given by the Fermi energy E_F of the Au electrodes.

To compute the electronic transmission function, we have employed an approach based on the combination of DFT and nonequilibrium Green's function techniques that we have interfaced to TURBOMOLE and explained in detail in Ref. [68]. Moreover, in order to correct for the known inaccuracies in DFT related to quasiparticle energies, we have made use of the DFT+Σ approach [65], which was implemented in our quantum transport method as described in Ref. [69].

In Fig. 8 we show our results for the electronic transmission τ_{el} as a function of energy for all the junctions in Figs. 2, 4, 6, and 7 based on both benzene and OPE3 derivatives. In all cases the electronic transport proceeds mainly through the tail of the highest occupied molecular orbital of the molecule in an off-resonant situation. The results for the transport properties of these molecular junctions at room temperature are summarized in Table I. We present there both the phononic and electronic thermal conductances κ_{pn} and κ_{el}, as well as the electrical conductance

$$G(T) = G_0 K_0(T), \quad \text{(A3)}$$

with $G_0 = 2e^2/h$. Moreover, when available, we also report the experimental values for G. The electric conductance can be used together with the Wiedemann-Franz law $\kappa_{el} \approx L_0 GT$ with the Lorentz number $L_0 = (k_B/e)^2\pi^2/3$ to estimate the electronic thermal conductance. We find the Wiedemann-Franz law to be approximately fulfilled for our computed molecular junctions, and the comparison of experimental and theoretical electrical conductance values G can hence be used to estimate uncertainties in the theoretical κ_{el}.

The key point is that in all the studied cases the electronic thermal conductance is considerably smaller than the corresponding phononic thermal conductance. In particular, for the junctions based on the benzene derivatives the electronic contribution is at least 5 times smaller than the phononic one, while for the OPE3 compounds the electronic contribution is more than two orders of magnitude smaller. Due to their lower G the longer molecules are thus advantageous if we want to exclude the contribution of electrons to heat transport.

TABLE I. Computed room-temperature phononic thermal conductance κ_{pn}, electronic thermal conductance κ_{el}, and electrical conductance G in units of the electrical conductance quantum $G_0 = 2e^2/h$ for the different molecular junctions investigated in this work. The last column shows, when available, the experimental value of the electrical conductance, as obtained from the peaks of conductance histograms. Experimental uncertainties due to broad distributions of conductance values have been omitted.

Molecule	κ_{pn} (pW/K)	κ_{el} (pW/K)	G (G_0) (theory)	G (G_0) (expt.)
1,4-diaminobenzene (para)	25.24	2.61	4.7×10^{-3}	6.4×10^{-3} [70]
2-fluoro-1,4-diaminobenzene	24.40	2.62	4.7×10^{-3}	5.8×10^{-3} [70]
2-chloro-1,4-diaminobenzene	22.17	2.70	4.9×10^{-3}	6.0×10^{-3} [70]
2-bromo-1,4-diaminobenzene	16.94	2.78	5.0×10^{-3}	6.1×10^{-3} [70]
2-iodo-1,4-diaminobenzene	15.24	3.25	5.8×10^{-3}	
2,5-dibromo-1,4-diaminobenzene	17.85	2.88	5.20×10^{-3}	
2,6-dibromo-1,4-diaminobenzene	10.46	2.88	5.19×10^{-3}	
2,3-dibromo-1,4-diaminobenzene	17.99	3.02	5.44×10^{-3}	
OPE3 (para)	24.57	0.11	1.94×10^{-4}	2.6×10^{-5} [71], 1.27×10^{-4} [72]
OPE3 (meta)	13.82	4.24×10^{-4}	7.53×10^{-7}	
F-OPE3	24.56	0.11	1.93×10^{-4}	
Cl-OPE3	23.12	0.11	1.96×10^{-4}	
Br-OPE3	19.62	0.11	1.97×10^{-4}	
I-OPE3	19.04	0.11	2.00×10^{-4}	

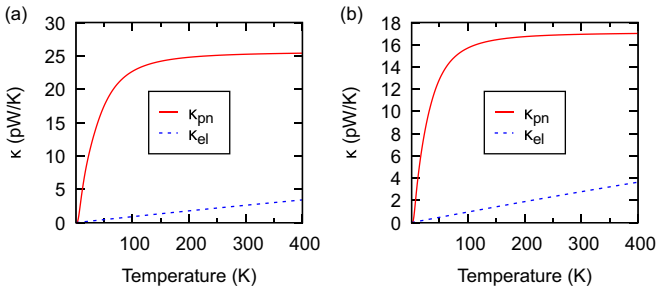

FIG. 9. Temperature dependence of the phononic and electronic contribution to the thermal conductance for the (a) Au-1,4-diaminobenzene-Au and (b) Au-2-bromo-1,4-diaminobenzene-Au junctions of Fig. 2.

Moreover, in order to illustrate that phonons dominate the thermal transport in these junctions for a wide temperature range, we show in Fig. 9 the temperature dependence of the phononic and electronic thermal conductances for the Au-1,4-diaminobenzene-Au and Au-2-bromo-1,4-diaminobenzene-Au junctions of Fig. 2. As one can see, the phononic contribution largely dominates at all temperatures between 10 and 400 K. Similar results hold for all the other molecular junctions.

To conclude, the results presented in this Appendix confirm that the thermal transport in the molecular junctions studied in this work is dominated by phonons. The predicted interference effects should therefore be visible in possible experiments.

[1] D. G. Cahill, P. V. Braun, G. Chen, D. R. Clarke, S. Fan, K. E. Goodson, P. Keblinski, W. P. King, G. D. Mahan, A. Majumdar, H. J. Maris, S. R. Phillpot, E. Pop, and L. Shi, Appl. Phys. Rev. **1**, 011305 (2014).

[2] M. Maldovan, Nat. Mater. **14**, 667 (2015).

[3] M. N. Luckyanova, J. Garg, K. Esfarjani, A. Jandl, M. T. Bulsara, A. J. Schmidt, A. J. Minnich, S. Chen, M. S. Dresselhaus, Z. Ren, E. A. Fitzgerald, and G. Chen, Science **338**, 936 (2012).

[4] J. Ravichandran, A. K. Yadav, R. Cheaito, P. B. Rossen, A. Soukiassian, S. J. Suresha, J. C. Duda, B. M. Foley, C.-H. Lee, Y. Zhu, A. W. Lichtenberger, J. E. Moore, D. A. Muller, D. G. Schlom, P. E. Hopkins, A. Majumdar, R. Ramesh, and M. A. Zurbuchen, Nat. Mater. **13**, 168 (2014).

[5] H. Han, L. G. Potyomina, A. A. Darinskii, S. Volz, and Y. A. Kosevich, Phys. Rev. B **89**, 180301 (2014).

[6] U. Fano, Phys. Rev. **124**, 1866 (1961).

[7] A. E. Miroshnichenko, S. Flach, and Y. S. Kivshar, Rev. Mod. Phys. **82**, 2257 (2010).

[8] B. Luk'yanchuk, N. I. Zheludev, S. A. Maier, N. J. Halas, P. Nordlander, H. Giessen, and C. T. Chong, Nat. Mater. **9**, 707 (2010).

[9] P. Fan, Z. Yu, S. Fan, and M. L. Brongersma, Nat. Mater. **13**, 471 (2014).

[10] J. C. Cuevas and E. Scheer, *Molecular Electronics: An Introduction to Theory and Experiment*, 2nd ed. (World Scientific, Singapore, 2017).

[11] P. Sautet and C. Joachim, Chem. Phys. Lett. **153**, 511 (1988).

[12] E. G. Emberly and G. Kirczenow, Phys. Rev. B **58**, 10911 (1998).

[13] R. Baer and D. Neuhauser, J. Am. Chem. Soc. **124**, 4200 (2002).

[14] R. Stadler, M. Forshaw, and C. Joachim, Nanotechnology **14**, 138 (2003).

[15] D. Walter, D. Neuhauser, and R. Baer, Chem. Phys. **299**, 139 (2004).

[16] D. M. Cardamone, C. A. Stafford, and S. Mazumdar, Nano Lett. **6**, 2422 (2006).

[17] C. A. Stafford, D. M. Cardamone, and S. Mazumdar, Nanotechnology **18**, 424014 (2007).

[18] S.-H. Ke, W. Yang, and H. U. Baranger, Nano Lett. **8**, 3257 (2008).

[19] D. Q. Andrews, G. C. Solomon, R. H. Goldsmith, T. Hansen, M. R. Wasielewski, R. P. V. Duyne, and M. A. Ratner, J. Phys. Chem. C **112**, 16991 (2008).

[20] G. C. Solomon, D. Q. Andrews, T. Hansen, R. H. Goldsmith, M. R. Wasielewski, R. P. V. Duyne, and M. A. Ratner, J. Chem. Phys. **129**, 054701 (2008).

[21] G. C. Solomon, D. Q. Andrews, R. H. Goldsmith, T. Hansen, M. R. Wasielewski, R. P. Van Duyne, and M. A. Ratner, J. Am. Chem. Soc. **130**, 17301 (2008).

[22] D. Q. Andrews, G. C. Solomon, R. P. Van Duyne, and M. A. Ratner, J. Am. Chem. Soc. **130**, 17309 (2008).

[23] R. Stadler, Phys. Rev. B **80**, 125401 (2009).

[24] G. C. Solomon, C. Herrmann, T. Hansen, V. Mujica, and M. A. Ratner, Nat. Chem. **2**, 223 (2010).

[25] T. Markussen, J. Schiøtz, and K. S. Thygesen, J. Chem. Phys. **132**, 224104 (2010).

[26] G. Géranton, C. Seiler, A. Bagrets, L. Venkataraman, and F. Evers, J. Chem. Phys. **139**, 234701 (2013).

[27] L. A. Zotti, E. Leary, M. Soriano, J. C. Cuevas, and J. J. Palacios, J. Am. Chem. Soc. **135**, 2052 (2013).

[28] A. Grigoriev, J. Sköldberg, G. Wendin, and Ž. Crljen, Phys. Rev. B **74**, 045401 (2006).

[29] T. A. Papadopoulos, I. M. Grace, and C. J. Lambert, Phys. Rev. B **74**, 193306 (2006).

[30] M. Ernzerhof, J. Chem. Phys. **127**, 204709 (2007).

[31] X. Shi, Z. Dai, and Z. Zeng, Phys. Rev. B **76**, 235412 (2007).

[32] C. M. Finch, V. M. García-Suárez, and C. J. Lambert, Phys. Rev. B **79**, 033405 (2009).

[33] K. Yoshizawa, T. Tada, and A. Staykov, J. Am. Chem. Soc. **130**, 9406 (2008).

[34] T. Markussen, R. Stadler, and K. S. Thygesen, Nano Lett. **10**, 4260 (2010).

[35] K. G. L. Pedersen, M. Strange, M. Leijnse, P. Hedegård, G. C. Solomon, and J. Paaske, Phys. Rev. B **90**, 125413 (2014).

[36] M. H. Garner, G. C. Solomon, and M. Strange, J. Phys. Chem. C **120**, 9097 (2016).

[37] M. Mayor, H. B. Weber, J. Reichert, M. Elbing, C. von Hänisch, D. Beckmann, and M. Fischer, Angew. Chem., Int. Ed. **42**, 5834 (2003).

[38] D. Fracasso, H. Valkenier, J. C. Hummelen, G. C. Solomon, and R. C. Chiechi, J. Am. Chem. Soc. **133**, 9556 (2011).

[39] W. Hong, H. Li, S.-X. Liu, Y. Fu, J. Li, V. Kaliginedi, S. Decurtins, and T. Wandlowski, J. Am. Chem. Soc. **134**, 19425 (2012).

[40] C. M. Guedon, H. Valkenier, T. Markussen, K. S. Thygesen, J. C. Hummelen, and S. J. van der Molen, Nat. Nanotechnol. **7**, 305 (2012).
[41] S. V. Aradhya, J. S. Meisner, M. Krikorian, S. Ahn, R. Parameswaran, M. L. Steigerwald, C. Nuckolls, and L. Venkataraman, Nano Lett. **12**, 1643 (2012).
[42] H. Vazquez, R. Skouta, S. Schneebeli, M. Kamenetska, R. Breslow, L. Venkataraman, and M. Hybertsen, Nat. Nanotechnol. **7**, 663 (2012).
[43] V. Rabache, J. Chaste, P. Petit, M. L. Della Rocca, P. Martin, J.-C. Lacroix, R. L. McCreery, and P. Lafarge, J. Am. Chem. Soc. **135**, 10218 (2013).
[44] C. R. Arroyo, S. Tarkuc, R. Frisenda, J. S. Seldenthuis, C. H. M. Woerde, R. Eelkema, F. C. Grozema, and H. S. J. van der Zant, Angew. Chem., Int. Ed. **52**, 3152 (2013).
[45] C. R. Arroyo, R. Frisenda, K. Moth-Poulsen, J. S. Seldenthuis, T. Bjørnholm, and H. S. J. van der Zant, Nanoscale Res. Lett. **8**, 234 (2013).
[46] J. Xia, B. Capozzi, S. Wei, M. Strange, A. Batra, J. R. Moreno, R. J. Amir, E. Amir, G. C. Solomon, L. Venkataraman, and L. M. Campos, Nano Lett. **14**, 2941 (2014).
[47] D. Z. Manrique, C. Huang, M. Baghernejad, X. Zhao, O. A. Al-Owaedi, H. Sadeghi, V. Kaliginedi, W. Hong, M. Gulcur, T. Wandlowski, M. R. Bryce, and C. J. Lambert, Nat. Commun. **6**, 6389 (2015).
[48] R. Frisenda, V. A. E. C. Janssen, F. C. Grozema, H. S. J. van der Zant, and N. Renaud, Nat. Chem. **8**, 1099 (2016).
[49] T. Markussen, J. Chem. Phys. **139**, 244101 (2013).
[50] M. Famili, I. Grace, H. Sadeghi, and C. J. Lambert, Chem. Phys. Chem. **18**, 1234 (2017).
[51] Q. Li, I. Duchemin, S. Xiong, G. C. Solomon, and D. Donadio, J. Phys. Chem. C **119**, 24636 (2015).
[52] L. Cui, W. Jeong, S. Hur, M. Matt, J. C. Klöckner, F. Pauly, P. Nielaba, J. C. Cuevas, E. Meyhofer, and P. Reddy, Science **355**, 1192 (2017).
[53] N. Mosso, U. Drechsler, F. Menges, P. Nirmalraj, S. Karg, H. Riel, and B. Gotsmann, Nat. Nanotechnol. **12**, 430 (2017).
[54] A. Jain and A. J. H. McGaughey, Phys. Rev. B **93**, 081206 (2016).
[55] M. Bürkle, T. J. Hellmuth, F. Pauly, and Y. Asai, Phys. Rev. B **91**, 165419 (2015).
[56] J. C. Klöckner, M. Bürkle, J. C. Cuevas, and F. Pauly, Phys. Rev. B **94**, 205425 (2016).
[57] J. C. Klöckner, R. Siebler, J. C. Cuevas, and F. Pauly, Phys. Rev. B **95**, 245404 (2017).
[58] TURBOMOLE GmbH, TURBOMOLE, http://www.turbomole.com. TURBOMOLE was a development of the University of Karlsruhe and Forschungszentrum Karlsruhe from 1989 to 2007, and development has been undertaken by TURBOMOLE GmbH since 2007.
[59] P. Deglmann, F. Furche, and R. Ahlrichs, Chem. Phys. Lett. **362**, 511 (2002).
[60] P. Deglmann, K. May, F. Furche, and R. Ahlrichs, Chem. Phys. Lett. **384**, 103 (2004).
[61] J. P. Perdew and Y. Wang, Phys. Rev. B **45**, 13244 (1992).
[62] J. P. Perdew, K. Burke, and M. Ernzerhof, Phys. Rev. Lett. **77**, 3865 (1996).
[63] F. Weigend and R. Ahlrichs, Phys. Chem. Chem. Phys. **7**, 3297 (2005).
[64] F. Weigend, Phys. Chem. Chem. Phys. **8**, 1057 (2006).
[65] S. Y. Quek, L. Venkataraman, H. J. Choi, S. G. Louie, M. S. Hybertsen, and J. B. Neaton, Nano Lett. **7**, 3477 (2007).
[66] H.-W. Lee, Phys. Rev. Lett. **82**, 2358 (1999).
[67] M. T. González, X. Zhao, D. Z. Manrique, D. Miguel, E. Leary, M. Gulcur, A. S. Batsanov, G. Rubio-Bollinger, C. J. Lambert, M. R. Bryce, and N. Agraït, J. Phys. Chem. C **118**, 21655 (2014).
[68] F. Pauly, J. K. Viljas, U. Huniar, M. Häfner, S. Wohlthat, M. Bürkle, J. C. Cuevas, and G. Schön, New J. Phys. **10**, 125019 (2008).
[69] L. A. Zotti, M. Bürkle, F. Pauly, W. Lee, K. Kim, W. Jeong, Y. Asai, P. Reddy, and J. C. Cuevas, New J. Phys. **16**, 015004 (2014).
[70] L. Venkataraman, Y. S. Park, A. C. Whalley, C. Nuckolls, M. S. Hybertsen, and M. L. Steigerwald, Nano Lett. **7**, 502 (2007).
[71] M. T. González, A. Díaz, E. Leary, R. García, M. A. Herranz, G. Rubio-Bollinger, N. Martín, and N. Agraït, J. Am. Chem. Soc. **135**, 5420 (2013).
[72] Q. Lu, K. Liu, H. Zhang, Z. Du, X. Wang, and F. Wang, ACS Nano **3**, 3861 (2009).